Turkish Journal of Electrical Engineering & Computer Sciences

http://journals.tubitak.gov.tr/elektrik/

Research Article

Turk J Elec Eng & Comp Sci
(2015) 23: 1715 – 1734

doi:10.3906/elk-1403-295

The integrated control of fuzzy logic and model-based approach for variable-speed wind turbine

Jian YANG[1], Dongran SONG[1,*], Hua HAN[1], Pengsha TONG[2], Ling ZHOU[2]
[1]School of Information Science and Engineering, Central South University, Changsha, P.R. China
[2]Chinese Ming Yang Wind Power Group Co., Ltd., Zhongshan, P.R. China

Received: 29.03.2014 • **Accepted/Published Online:** 12.03.2015 • **Printed:** 30.11.2015

Abstract: For a variable-speed wind turbine (VSWT), the primary objective of control is to maximize power generation while maintaining the desired rotor speed and avoiding equipment overloads. To fulfill the control objectives, the classical model-based control (MBC) has been widely used, which refers to two controllers: torque controller (TC) and pitch controller (PC). In this work, the drawbacks of MBC for VSWTs are studied extensively. It reveals that there are transition issues between the TC and PC, and over-speed problems under large turbulent wind when only MBC is taken. To improve the control performance of the VSWT, an integrated control solution is presented, in which three fuzzy logic control modules are designed to function in parallel with MBC modules. Potential integrated structures are also given and a structure suitable for industrial application is adopted in this study. The proposed solution is applied to update the raw control system of a 3.0 MW VSWT of the Chinese Ming Yang Wind Power, which is validated with nonlinear simulations by using the commercial wind turbine simulation tool Bladed in accordance with IEC standards. The results prove that good performance of the target wind turbine is guaranteed under the proposed integrated control structure.

Key words: Variable-speed wind turbine, integrated control, model-based control, fuzzy logic control

1. Introduction

Wind energy is a renewable energy with fast-growing utilization. According to the World Wind Energy Association, the worldwide wind capacity reached 336,327 MW by the end of June 2014, out of which 17,613 MW was added in the first 6 months of 2014 [1]. Despite the amazing growth in the capacity of wind turbine (WTs), there are still challenges for engineering and science. Modern WTs are variable-speed, large, flexible structure operating in uncertain environments and possibly lend themselves to different and diverse control solutions. From the viewpoint of control theory, all control solutions are categorized as one of two methods: model-based control (MBC), referring to classical control and modern control, and model-free control (MFC), referring to intelligent control and theory of large-scale systems [2].

Among MBC for WTs, proportional-integral-differential (PID) control and linear-quadratic-Gaussian (LQG) control are the approaches demonstrated to be effective in industrial applications [3,4]. The classical PID control is the only approach for controlling WTs at the beginning, since, as we know, PID control can be designed and tuned by trial-and-error. Later, with more understanding of the dynamics of WTs, the single-in-single-out (SISO) linearized model of a WT was presented to design PID parameters [5–8]. For WTs, the primary objective of control is to maximize power generation while maintaining the desired rotor speed and

*Correspondence: humble_szy@163.com

avoiding equipment overloads [9]. The PID approach [10–14] is widely used in such a case. The secondary objective is to alleviate fatigue load, and the LQG approach has success [11–13] in such a scenario. However, the LQG approach is based on the state-space model and requires additional states and variables for defining the quadratic cost function, which bring difficulties in industrial application. Moreover, the definition of suitable cost function is not so straightforward. Thereafter, PID has for the most part been used in wind energy industry, with its advantages of being simple to implement, easy for dealing with nonlinearity through techniques such as gain scheduling, and straightforward for adjustments such as the addition of filters [15].

While the wind energy industry has continuously been using MBC approaches, MFC solutions to WTs are drawing more and more attention from both communities of control theory research and wind energy industry in recent years. As an important branch of intelligent control, fuzzy logic control (FLC) has been proposed to get better power production and speed stability under the primary objectives. In [16], fixing the voltage amplitude for loads supplied from a hybrid energy system, a type-1 FLC and PI-controller were designed and compared to each other. Since the normal design of the FLC system is completely based on the knowledge and experience of designers, a neuro-fuzzy-based control technique was proposed to automatically tune the memberships of FLC [17], controlling generator speed and power. In order to handle nonlinearities and uncertainties of WTs, much research has been conducted, as follows: interval type-2 fuzzy controllers and an adaptive fuzzy controller with self-tuning fuzzy sliding-mode compensation were proposed to design the pitch controller (PC) in [18] and [19], respectively; an adaptive proportional-integral (PI) controller for optimal power control was also studied, for which optimal gains of the torque controller (TC) are derived via particle swarm optimization algorithm and FLC theory, in [20]. Meanwhile, fuzzy-based models were introduced to represent the nonlinear behavior of WTs: a fuzzy model-based multivariable predictive control strategy, based on the Takagi–Sugeno fuzzy model of WTs, was developed to maintain constant power output while minimizing variations of generator speed and pitch angle [21]. For maximizing energy extraction from WTs, Takagi–Sugeno–Kang fuzzy models were generated from data-driven design methodologies [22]. Moreover, FLC has already been integrated with other intelligent control theories to design adaptive interference models. For example, in [23], an adaptive neuro-fuzzy inference system was designed for controlling output voltage and frequency of a variable-speed wind power generation system.

In general, regarding the above studies, their motivations originated from considering the nonlinear nature of WTs and uncertainties of models. Thereafter, FLC-based or FLC-involved approaches were proposed to bypass the need for precise linearized models. Among them, some promising results have been shown. However, none of them were validated with detailed nonlinear simulations using three-dimensional turbulent wind inputs, which are vital to verify the design before implementing it on a real turbine [10]. In addition, the degree of difficulty in implementing adaptive FLC in engineering applications was not evaluated. To some extent, more advanced FLC requires more effort to be designed and simulated, not to mention carrying out the field trials. From the viewpoint of industrial application, controls of WTs are required to be practical and easy to implement. Focusing on industrial applications, this study aims to propose FLC solutions to assist MBC rather than replace it. It answers the following questions: Are there some issues that MBC solutions fail to cover? What are the reasons for these failures? How can we resolve these problems while maintaining the advantages of MBC?

According to authors' experience in the wind energy industry, there are two specific issues to handle: the cooperation and switching between the TC and PC, and the over-speed problem easily caused by large amounts of turbulent wind. With regards to MBC, the cooperation and switching of the TC and PC is not a standard

control problem [24]. Wright and Fingersh [7,8], from the National Renewable Energy Laboratory, introduced a Region 2.5 and some simple logic to decouple the TC and PC; engineers from GE Power Systems added one more PI controller into the PC [9]; and Bossanyi from Garrad Hassan proposed two additional bias terms for the TC and PC, respectively [10]. Bongers also proposed multiple linear controllers to achieve minimization of switching phenomena [25]. The over-speed issue easily caused by large-scale turbulence is related to the PC. To solve this problem, an ideal approach is to consider wind velocity as an input to design a feed-forward term. However, this solution requires the additional measure of a LIDAR sensor, which brings higher costs and is only applied in some research projects currently [26,27]. As an alternative in application, an additional nonlinear pitch control term was mentioned in [13], but detailed information was not given for the sake of proprietary rights.

To the best of our knowledge, these two issues are mainly solved through trial and error by engineers. Although solutions to the above two issues are various, few of them are designed with certain methodology. This work aims to develop a systematic solution in which FLC modules are well integrated with MBC parts, and can therefore be used in the wind energy industry. This study is structured as follows. In Section 2, the basic control system structure of the WT together with MBC designs is introduced and analyzed; in Section 3, the mentioned two issues uncovered by MBC are discussed and three type-1 FLC modules are proposed to handle them; in Section 4, potential integration structures of FLC and MBC are developed; in Section 5, the proposed solution is applied to the raw controller of a 3 MW WT, and the improved performance of the WT is validated with nonlinear simulations; and, finally, conclusions are drawn in Section 6.

2. MBC of WT

2.1. Basic control system structure

A basic control system structure of the WT is shown in Figure 1, where v stands for wind velocity; w_r and w_g denote rotor speed and generator speed, respectively; T_r and T_g refer to aerodynamic torque and generator torque, respectively; θ_{mes} and w_{mes} represent measured pitch angle and generator speed (or rotor speed), respectively; and θ_{cmd} and T_{cmd} are pitch angle command and generator torque command from the control system, respectively.

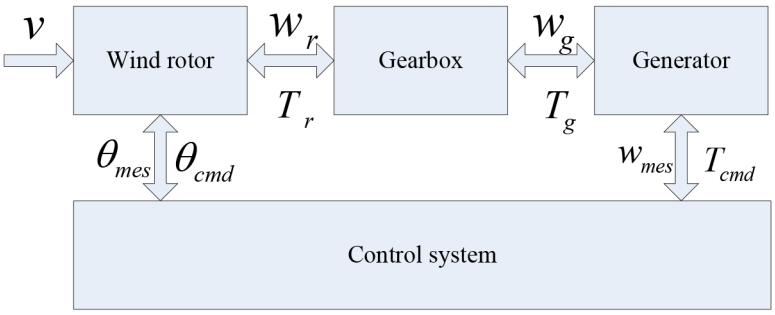

Figure 1. Block diagram of the WT's control system.

From Figure 1, it is clear that there are two pairs of inputs and outputs available: θ_{cmd} and θ_{mes}, T_{cmd} and w_{mes}. Ignoring physical constraints, it is natural to consider the system as a two-input, two-output structure. Moreover, more state variables can be obtained when internal couplings among subcomponents of the WT such as blades, yawing system, drive train, and tower are considered. Thereafter, multivariable state-space models can be obtained to design controllers involving primary and secondary objectives [7,8].

This study only concerns the mentioned primary objective; thus, only the relation among variables shown in Figure 1 is used to model WT.

2.2. Linearized model

In Figure 1, the most important kinetic equation is given by Eq. (1); in that case, a single degree of freedom is presumed.

$$\dot{w}_r = (T_r - T_g N_{gear})/J, \tag{1}$$

where J is the inertia of WT and N_{gear} denotes the gearbox ratio. T_r is given by

$$T_r = P_r/w_r = C_p(\theta, v, w_r)\rho\pi R^2 v^3/(2w_r), \tag{2}$$

where P_r represents power captured by WT, ρ is air density, R denotes turbine radius, θ stands for pitch angle, and $C_p(\theta, v, w)$ refers to the power coefficient as a function of θ, v, and w_r.

Referring to Eq. (2), a basic kinetic equation of the WT is given by

$$\dot{w}_r = (T_r(\theta, v, w_r) - T_g N_{gear})/J. \tag{3}$$

In Eq. (3), T_r is a nonlinear function of θ, v, and w_r. In order to facilitate controller designs, it has to be linearized. Since T_r is a continuous function of θ, v, and w_r, it is approximated as

$$T_r \approx T_r(w_{r0}, v_0, \theta_0) + (\partial T_r/\partial w_r)\delta w_r + (\partial T_r/\partial v)\delta v + (\partial T_r/\partial \theta)\delta\theta. \tag{4}$$

Being a function of w_r in some way, T_g is simplified as

$$T_g \approx T_g(w_{r0}) + (\partial T_g/\partial w_r)\delta w_r. \tag{5}$$

In Eqs. (4) and (5), variables with the suffix 0 represent the linearization point and variables with suffix δ denote perturbations at equilibrium. Combining Eqs. (3)–(5), the rotor speed error is expressed as

$$\delta\dot{w}_r = [(\partial T_r/\partial w_r)\delta w_r + (\partial T_r/\partial v)\delta v + (\partial T_r/\partial \theta)\delta\theta - (\partial T_g/\partial w_r)\delta w_r N_{gear}]/J. \tag{6}$$

For simplicity, use a, b, c, and d to denote $\partial T_r/\partial w_r, \partial T_r/\partial v, \partial T_r/\partial\theta$, and $\partial T_g/\partial w_r$, respectively, and Eq. (6) is then changed to:

$$\delta\dot{w}_r = (a\delta w_r + b\delta v + c\delta\theta - d\delta w_r N_{gear})/J. \tag{7}$$

Eq. (7) is the linearized model with parameters a, b, c, and d, which are determined by the linearization point. Based on this model, a systematic MBC design is introduced in the following sections.

2.3. Formulation of primary objectives

For the WT, the primary objectives of control are to maximize power production, maintain the desired rotor speed, and avoid equipment overloads. These objectives are formulated as an optimal problem under certain constraints, which is governed by

$$\begin{array}{l} \min |P_g - P_{opt}| \\ s.t.\{w_g \in [0, w_{g\_rated}], T_g \in [0, T_{g\_rated}], \theta \in [\theta_{\min}, \theta_{\max}]\} \end{array}, \tag{8}$$

where P_g is output power from generator and P_{opt} denotes optimal power. In this study, assume that power loss of the WT is negligible, and thus P_g equates to P_r.

From Eq. (2), obviously P_r is maximized when $C_p(\theta, v, w)$ is optimal. Thanks to the good design of modern blades, $C_p(\theta, v, w)$ has the following characteristics:

- There is only one maximal $C_p(\theta, v, w)$ for each θ, solved by tracking the set of (v, w_r);
- There is a single optimal pitch angle matching the global maximal $C_p(\theta, v, w)$, called fine pitch θ_{fine};
- There is monotone decreasing of $C_p(\theta, v, w)$ in terms of θ.

Thereafter, the primary objectives are divided into two parts as follows:

$$\begin{array}{l} \min |w_r - w_{opt}| \\ s.t.\{T_g \in [0, T_{g\_rated}], \theta = \theta_{fine}\} \end{array}, \tag{9}$$

and

$$\begin{array}{l} \min |w_r - w_{r\_rated}| \\ s.t.\{T_g = T_{g\_rated}, \theta \in [\theta_{fine}, \theta_{\max}]\} \end{array}. \tag{10}$$

From Eqs. (9) and (10), it is obvious that the primary objectives are fulfilled by controlling rotor speed w_r:

- The control objective is to track the optimal value w_{opt} before T_g reaches the rated value;
- The control objective is to keep w_r at the rated value once the rated torque is reached.

2.4. MBC design

With the objective functions of Eqs. (9) and (10), and the linearized model of Eq. (7), we reach the MBC design. Eq. (9) only involves the output variable, generator torque, and thus the related controller is normally called a TC. Similarly, Eq. (10) is related to a so-called PC.

2.4.1. TC design

Considering Eq. (9), the control objective is to track w_{opt}. However, w_{opt} is determined by v, which means that the reference to w_r varies all the time. The equilibrium point barely exists, and thus the MBC design approach based on the linearized mode of Eq. (7) is not quite reasonable.

In industrial applications, controller designs for the objective function of Eq. (9) are based on the tip speed ratio method [13,28] or the query table methodology [14,28]. Both of them originate from the calculation of optimal $C_p(\theta, v, w)$, with difference in processes. For simplification, the query table method is applied as

$$T_{g\_cmd} = T(w_{g\_mes}), \forall\{w_{g\_mes} \in (0, w_{g\_\max})\}, \tag{11}$$

where $T(w_{g\_mes})$ is a query table function, which is preset according to the optimal power curve normally provided by the manufacturer of WT. In Eq. (11), w_g and T_g can also be replaced by w_r and P_g, respectively.

2.4.2. PC design

Considering Eq. (10), the control objective is to keep w_r at the rated value while maintaining generator torque at the rated value. Here, a MBC approach based on the linearized model of Eq. (7) is adopted. Assuming that w_r keeps the rated value and v is a constant, Eq. (7) is simplified as

$$\delta\dot{w}_r = (c\delta\theta - d\delta w_r N_{gear})/J, \tag{12}$$

where δw_r is controlled through adjusting $\delta\theta$, and thus the pitch actuator should be modeled. In this study, the pitch actuator's output is considered as pitch speed command $\delta\dot{\theta}_{cmd}$ and its model is given by

$$\delta\dot{\theta}_{cmd}/\delta\theta = s/e^{-\tau s} \approx (1+\tau s)s, \tag{13}$$

where τ is the delay time of the pitch actuator.

Recalling Eqs. (12) and (13), the transfer function from $\delta\dot{\theta}_{cmd}$ to δw_r is obtained as

$$G_0(s) = \delta w_r/\delta\dot{\theta}_{cmd} = c/[s(1+\tau s)(Js + dN_{gear})]. \tag{14}$$

When the generator torque is kept at the rated value, d is zero and Eq. (14) is reduced to

$$G_0(s) = c/[Js^2(1+\tau s)]. \tag{15}$$

Eq. (15) describes a typical three-order model. According to classical control theory [29], the desired open-loop transfer function of a three-order system is

$$G_d(s) = K(T_1 S + 1)/[s^2(T_2 + 1)]. \tag{16}$$

Obviously, a PD controller satisfies construction of the desired transfer function, which is given by

$$G_c(s) = \delta\dot{\theta}_{cmd}/(w_{rated} - w_r) = -(k_p + k_d s). \tag{17}$$

By integrating Eqs. (15) and (17), the open-loop transfer function of the system including the PD part is given as

$$G(s) = G_c(s)G_0(s) = -(cK_p/J)(1 + K_d/K_p s)/[s^2(1+\tau s)]. \tag{18}$$

Some engineering design methods, such as three-order best design and minimal M_r design [29], are available to choose parameters of the transfer function of Eq. (18). Here, the minimal M_r design method is utilized and the PD parameters are chosen as

$$K_d/K_p = H\tau, cK_p/J = -(H+1)/2H^2\tau^3, \tag{19}$$

where H is a real number and its value ranges from 3 to 10.

For Eq. (19), there are two points worth noticing:

- Candidates of K_p and K_d are functions of c (or $\partial T_r/\partial\theta$), and thus they are gain-scheduling along with linearization points (similar technology was presented in [30]);
- The stability of the system requires a negative value of c, which is actually a requirement satisfied by the design of blades.

3. Specific issues of MBC and FLC solutions

3.1. Specific issues of MBC

The MBC presented in Section 2 matches the general requirement of primary control objectives for WTs. However, there are two specific issues that MBC cannot resolve: the transition issue between the TC and PC, and over-speed problem caused by large turbulent wind or gusts.

3.1.1. The transition issue between TC and PC

The transition issue between the TC and PC involves rotor speed control, which can be elaborated on well by checking some equations from Section 2. From Eq. (3), it is obvious that rotor speed w_r is affected by pitch angle θ and generator torque T_g at the same time. This coupling issue is alleviated by dividing control objectives into Eqs. (9) and (10), but it remains in the TC and PC, as formulated by Eq. (11) and Eq. (17), respectively. Therefore, when generator speed is regulated by the PC, T_g will suffer from dip along with w_r decreasing under the rated value; $\delta\dot{\theta}_{cmd}$ results in unnecessary action of the pitch angle while generator speed is under the regulation of the TC.

3.1.2. Over-speed problem under MBC

The over-speed shutdown easily caused by large turbulence is the problem related to the PC with the model-based design. The design of the PD controller is based on the linearized model formulated by Eq. (15) and parameters are chosen at the linearization point in terms of stability and anti-interference. In that case, the wind velocity is considered as a disturbance damped by the close-loop control. Nevertheless, if wind velocity varies very fast or a gust happens, the PC would fail to regulate rotor speed promptly. As the result, a fast shutdown or even an emergence shutdown happens to the WT, reducing power generation and also resulting in a large mechanic load to the WT.

3.2. FLC solutions

3.2.1. FLC solutions to the transition issue

To decouple the TC and PC, the simplest solution is to introduce some logic rules to make the decision of whether w_r is controlled by the TC or the PC. However, the design of such logic rules requires expert knowledge. Here, the knowledge applied is summarized as follows:

- When the pitch angle is far above the fine pitch, $f(\theta)$ should make sure the generator power keeps the rated value;
- When the pitch angle is decreasing to the fine pitch, $f(\theta)$ should keep the generator power at the rated value for a while;
- When the generator power is far less than the rated value, $f(P)$ should make sure the pitch angle keeps the rated value;
- When the generator power is increasing to the rated value, $f(P)$ should make the pitch angle ready for action;

where $f(\theta)$ and $f(P)$ are additional outputs to the TC and PC, respectively.

Two FLC modules (named FLC1 and FLC2) are designed to output $f(\theta)$ and $f(P)$, for which the pitch angle and generator power are inputs, respectively. In theory, both type-1 and type-2 FLC are suitable for this case. Type-2 FLC outweighs type-1 FLC in handling uncertainty, but type-1 FLC is simpler to implement and straightforward for adjusting parameters during simulation and field trials. Type-1 FLC is recommended and adopted in this study.

3.2.2. FLC solution to the over-speed problem

As shown in Section 2.4.2, it is clear that fast and big wind disturbance is not considered in the design of the PC. Meanwhile, a modern WT has large inertia and there is delay time for the pitch actuators. Thereafter, the over-speed problem arises. To solve this problem, a FLC module (named FLC3) is proposed, for which rotor speed error and its derivative are inputs. The basic rules are listed as follows:

- $f(\bullet)$ only functions when rotor speed error and its derivative have the same sign;
- $f(\bullet)$ is big when rotor speed error and its derivative are big;
- $f(\bullet)$ is medium when rotor speed error and its derivative are medium;
- $f(\bullet)$ is small when rotor speed error is small and its derivative are medium;

where $f(\bullet)$ is the output of FLC3. Type-1 FLC is also adopted for FLC3 in this study.

4. The integration of FLC and MBC

FLC design is still more a matter of art than technology since there is no standard and systematic structure to define it [31]. In other words, the design of FLC is very flexible. In this study, the flexibility is embodied in the integration structure of FLC and MBC. The possible integration structures are shown in Figure 2. For FLC1, its output can be connected to position 1 or position 2 of the TC; for FLC2, its output can be connected to position 1 or position 2 of the PC; for FLC3, its output can be connected to position 1 or position 2 or position 3 of the PC.

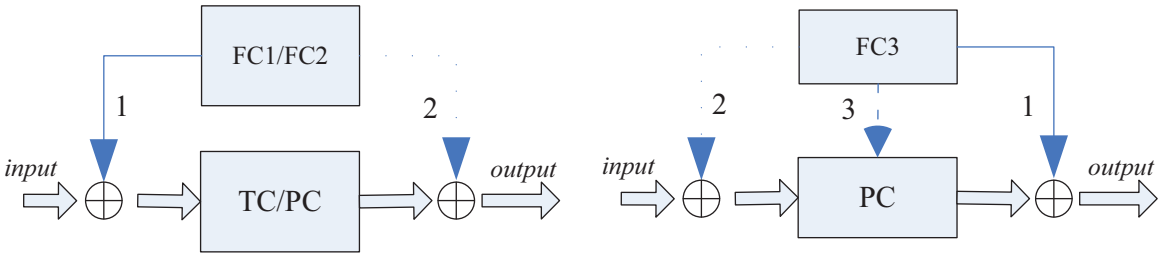

Figure 2. Possible integration structures of FLC and MBC.

Although these integration candidates can achieve the same goals, obviously the difficulties in designing them are different. Take FLC3, for example: at position 1, FLC3 is an independent controller, which operates in parallel with a PD controller; at position 2, FLC3 relies on the PD structure and it functions by adjusting the input of the PD controller; at position 3, PC parameters are adjusted by FLC3, and thus it is a variable-parameter PD controller as a whole. Similar situations happen with FLC1 and FLC2.

In this study, all outputs of FLC are connected to point 1. In that case, FLC3 does not interfere with the PD controller; meanwhile, the implementations of FLC1 and FLC2 are comparably simple.

5. An application case

The proposed integration solution of FLC and MBC is developed for a 3.0 MW WT of Chinese Ming Yang Wind Power (CMYWP). The objective of the application case is to improve the raw controller, which was designed by Freqcon GmbH in Germany. As the raw controller has already been used in some WTs, only the designing of the FLC modules is presented in this work. The raw controller of WT is easily updated without losing previous performance.

5.1. Basic information of the target WT

The target WT is a two-blade 3.0 MW super compact drive (SCD) machine designed by Aerodyn Energy System GmbH. Its specifications are shown in Table 1.

Table 1. Specification of target WT.

Parameters	Value
Rotor diameter	100 m
Number of rotor blades	2
Rated electrical power at grid connection point	3000 kW
Rotor speed range	6.0–21.0 rpm
Nominal rotor speed	17.1 rpm
Rated wind speed	12.9 m/s
Rotor moment of inertia	$1.1 \times 10^7 kg \bullet m^2$
Generator moment of inertia	$2.1 \times 10^3 kg \bullet m^2$
Gearbox ratio	23.94
Cut-in wind speed	3 m/s
Cut-out wind speed	25 m/s
Cut-out rotor speed	19.15 rpm
Activation rotor speed	20.5 rpm
Pitch system type	Hydraulic
Hardware limitation for pitch speed	$[-10, 10(\deg/s)]$
Hardware limitation for pitch angle	$[-0.5, 95(\deg)]$
Fine pitch position	0 deg
Response time of pitch actuator	0.1 s

The structure of the raw control system is shown in Figure 3 (the part inside the dashed box), where the scaling parts and filter parts are not included.

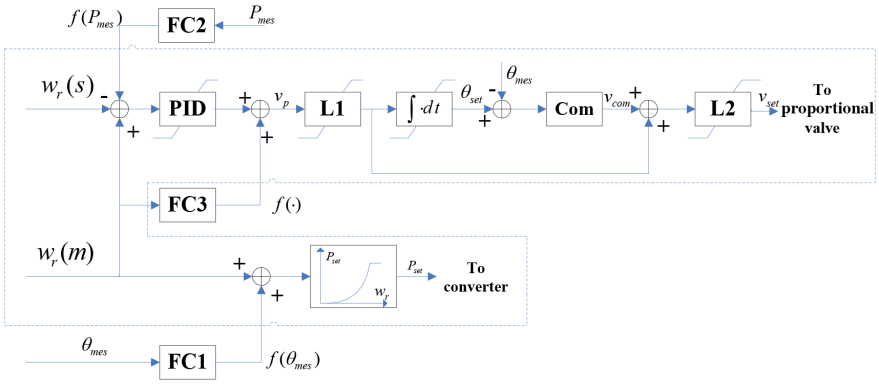

Figure 3. The structure of the control system under study.

For the PC part, a PD controller is used, for which the input is the error between the reference value $w_r(s)$ and the measured value $w_r(m)$ of rotor speed, and the output is the pitch speed set-value v_{set} to the proportional valve. The components L_1, L_2, and com are two limiters and one compensator, respectively. The parameters of the PD controller are shown in Table 2.

Table 2. The TC parameters.

Measured rotor speed (rpm)	Generator torque set-point (100%)
6.0	0.0
9.6	18.0
11.6	3.0
12.6	23.0
14.3	42.0
17.1	100.0
19.0	101.0
21.0	101.0

For the TC part, a lookup-table curve (generator-torque vs. rotor-speed) is used, in which eight pairs of interpolations are preset based on the optimum tip speed ratio and a tower exclusion zone is built up between 9.6 rpm and 11.6 rpm. The parameters of the TC are shown in Table 3.

Table 3. The PC parameters.

Measured pitch angle (deg)	P value	D value
0.0	0.8	2.0
5.0	0.768	1.92
12.0	0.735	1.84
20.0	0.694	1.74
30.0	0.64	1.6

5.2. FLC parts design under new control system structure

The whole structure of the new control system is shown in Figure 3. Together with the raw control structure, three new modules are added: FLC1, FLC2, and FLC3, with outputs $f(\theta)$, $f(P)$, and $f(\bullet)$, respectively. For these FLC modules, the output level ranges from NB to PB, where NB is negative big, NM is negative medium, NS is negative small, ZO is zero, PS is positive small, PM is positive medium, and PB is positive big. The crisp points of $f(\theta)$, $f(P)$, and $f(\bullet)$ are calculated using the center average defuzzifier method [2]. The ANFIS Edit software of the Fuzzy Logic Toolbox in MATLAB is used to design the FLC modules.

5.2.1. Module FLC1 design

For module FLC1, the measured pitch angle θ_{mes} is taken as the input and $f(\theta)$ is the output. The basic domain for θ_{mes} is set to $[0, 5(\text{deg})]$. The basic domain for $f(\theta)$ satisfies a constraint from rotor speed (or generator speed) to produced power. The constraint is determined by the capacity specifications of the generator and converter. In this study, it is set to $[0, 1.2(rpm)]$.

The membership functions for input and output sets are shown in Figures 4 and 5, respectively.

The control rules of FLC1 are presented in Table 4.

The control curve from θ_{mes} to $f(\theta)$ is shown in Figure 6.

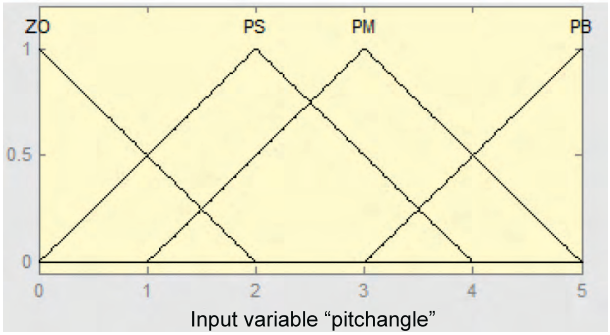

Figure 4. Membership function of θ_{mes}.

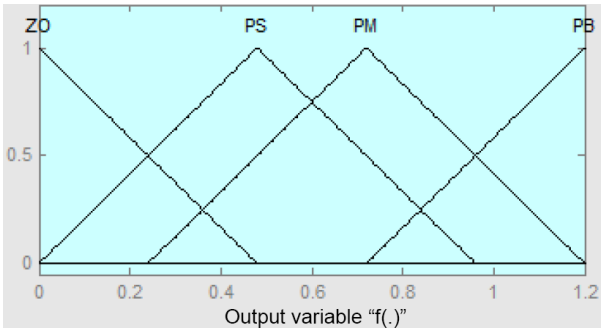

Figure 5. Membership function of $f(\theta)$.

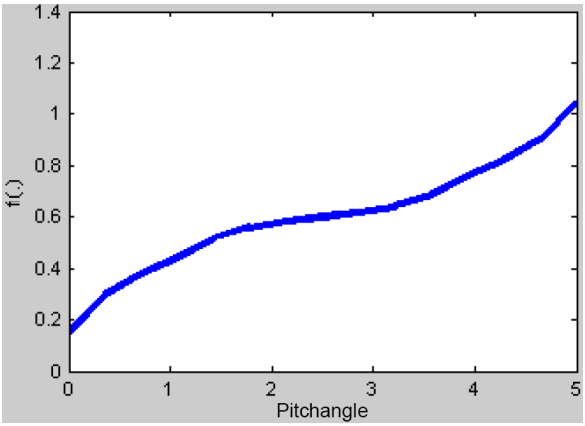

Figure 6. Control curve from θ_{mes} to $f(\theta)$.

Table 4. The rule base of FLC1.

θ_{mes}	ZO	PS	PM	PB
$f(\theta)$	ZO	PS	PM	PB

5.2.2. Module FLC2 design

For module FLC2, the measured power P_{mes} is the input and $f(P)$ is the output. The basic domains are $[0.9, 1.0(p.u.)]$ and $[0, 2.0(rpm)]$ for P_{mes} and $f(P)$, respectively. The membership functions for both input and output sets are shown in Figures 7 and 8, respectively.

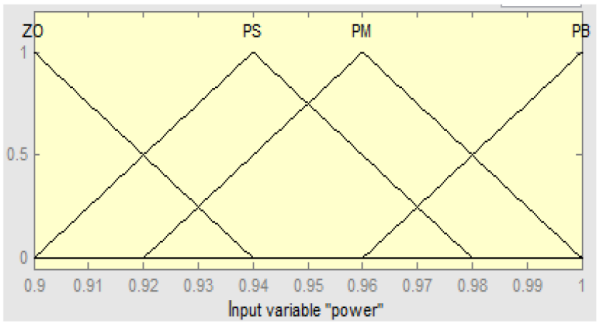

Figure 7. Membership function of P_{mes}.

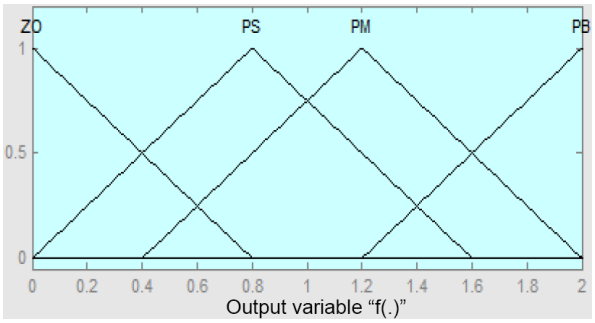

Figure 8. Membership function of $f(P)$.

The control rules of FLC2 are presented in Table 5.

The corresponding control curve from P_{mes} to $f(P)$ is shown in Figure 9.

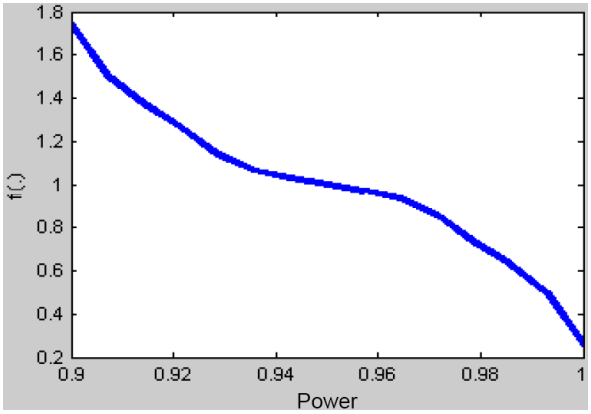

Figure 9. Control curve from P_{mes} to $f(P)$.

Table 5. The rule base of FLC2.

P_{mes}	ZO	PS	PM	PB
$f(P)$	PB	PM	PS	ZO

5.2.3. Module FLC3 design

For module FLC3, two inputs are rotor speed error E and its derivative E_c. The basic domains of E and E_c are set to $[-0.06, 0.06(p.u.)]$ and $[-0.06, 0.06(rad/s^2)]$, respectively. The basic domain for $f(\bullet)$ is set to $[-2, 2(\deg/s)]$. The membership functions for input and output sets are shown in Figures 10–12, respectively.

The control rules of FLC3 are presented in Table 6.

The corresponding three-dimensional control surface is shown in Figure 13.

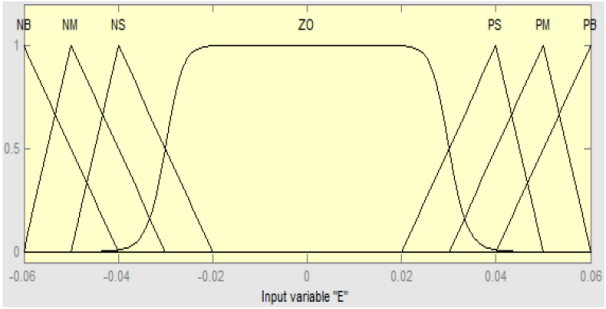

Figure 10. Membership function of E.

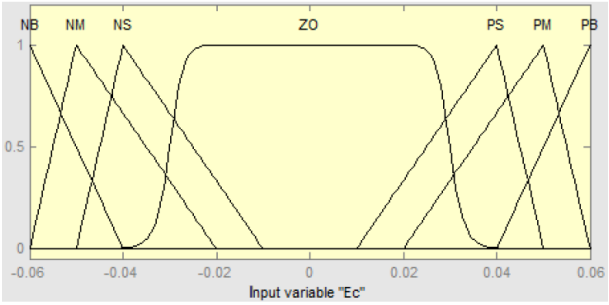

Figure 11. Membership function of E_c.

5.3. Simulation test and results analysis

For testing the proposed integration solution of FLC and MBC, the industry-standard software for WT performance and loading calculations, Garrad Hassan's Bladed [32] wind turbine software package, is used to carry out simulations. The source codes of the raw controller and two updated controllers are developed as an external dynamic link library to the model of the WT. Detailed simulations are carried out in accordance with IEC 61400-1 [33] and the wind turbulence density is set to 18%.

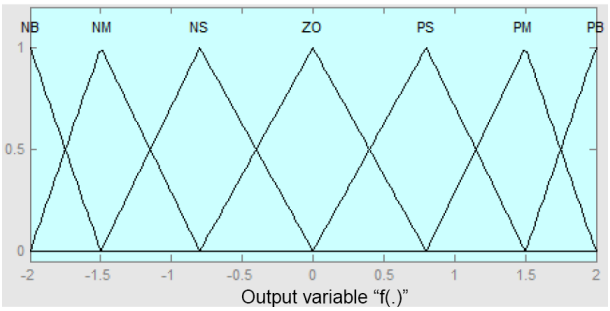

Figure 12. Membership function of $f(\bullet)$.

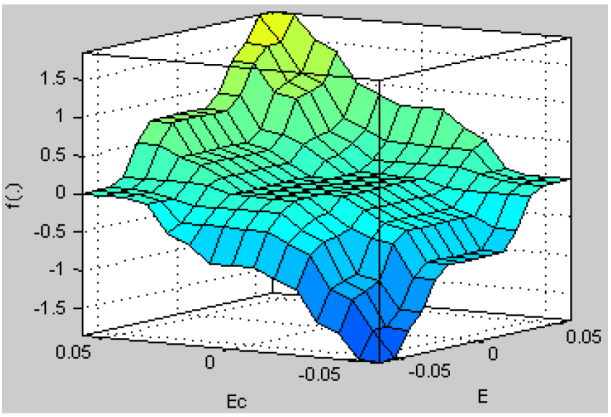

Figure 13. Control surface from E and E_c to $f(\bullet)$.

Table 6. The rule base of FLC3.

$f(\cdot)$		E						
		NB	NM	NS	ZO	PS	PM	PB
E_c	NB	NB	NB	NM	NS	ZO	ZO	ZO
	NM	NB	NM	NM	NS	ZO	ZO	ZO
	NS	NM	NS	NS	ZO	ZO	ZO	ZO
	ZO	NS	ZO	ZO	ZO	ZO	ZO	PS
	PS	ZO	ZO	ZO	ZO	PS	PS	PM
	PM	ZO	ZO	ZO	PS	PM	PM	PB
	PB	ZO	ZO	ZO	PS	PM	PB	PB

In order to illustrate the advantages of the proposed solution, three types of controller are simulated and compared: the raw controller, the proposed controller in the study, and another updated controller improved by conventional strategy. The conventional strategy adopts the logic proposed in [7,8] to handle the transition issue and an additional nonlinear pitch control term to manage the over-speed problem according to [13]. The logic is set as follows: the rotor speed to produce rated power is decreased from 17.1 rpm to 16.9 rpm; when the rotor speed is higher than 16.9 rpm, the generator torque is set to stay constant. The relevant parameters for the nonlinear pitch control term are as follows: time constant for the first order lag is 0.05s, scale factor for speed error is 0.628 rad/s, scale factor for change rate of speed error is 0.0157 rad/s^2, and gain is 0.21 rad/s.

Some representative simulation results are shown, which are based on 12 m/s and 20 m/s mean wind speed under design load case (DLC) 1.2, and extreme operational gusts at 13 m/s and 25 m/s under DLC 1.6. Among numerous simulation results obtained from the Data View menu of Bladed, four measured signals are drawn: wind speed, rotor speed, electrical power, and blade 1 pitch angle.

5.3.1. Results comparison between raw controller and proposed controller

Among simulation results, red curves result from the new controller and black ones are from the raw controller.

The simulation results at 12 m/s and 20 m/s mean wind speed are shown in Figures 14a and 14b, respectively. It is obvious that primary objectives are basically achieved for both the raw controller and proposed controller. However, the performance of the WT with the raw controller suffers from the transition issue: when rotor speed varies around the rated value (17.1 rpm), electrical power also deviates from rated power (3.0 MW);

even when sufficient wind is available and pitch angle is far away from fine pitch, there is still deep reduction of output power and unnecessary pitch angle reserves when generator power is less than 3.0 MW. In contrast, the WT with updated controller shows much better performance: there is almost no power reduction and generator power keeps tightly to 3.0 MW as long as the pitch angle is reserved; meanwhile, rotor speed is less over-shot when the controller transitions from the TC to PC (checking the rotor speed at about 130 s in Figure 14a); moreover, rotor speed becomes concentrated in the range of 16.6–17.6 rpm when wind speed is higher than the rated value (12.9 m/s).

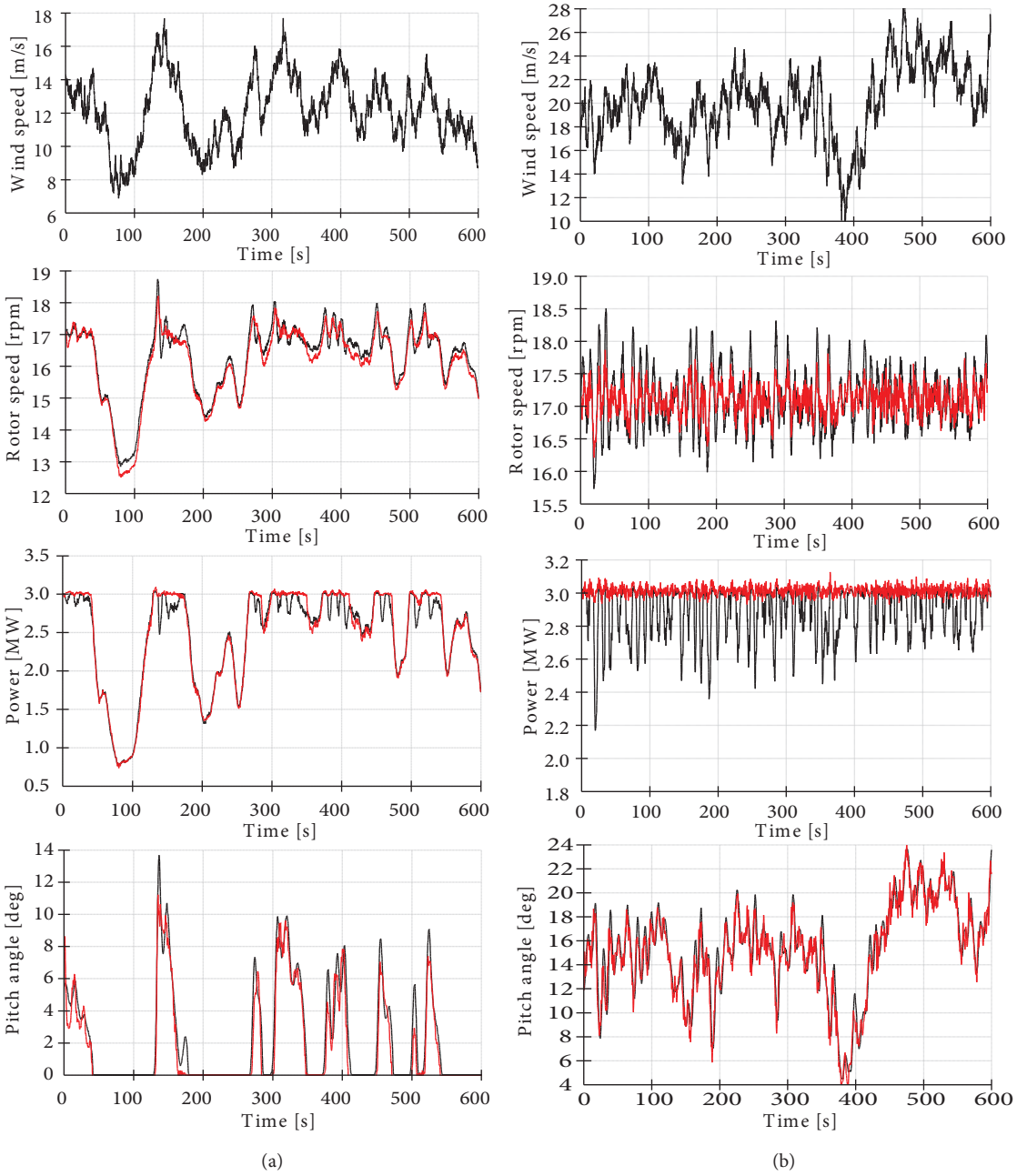

Figure 14. Simulation results under DLC 1.2 between raw controller and proposed controller (a) at wind speed of 12 m/s and (b) at wind speed of 20 m/s.

Figures 15a and 15b show simulation results under extreme operational gusts at 13 m/s and 25 m/s, respectively. The rotor-speed maximum values of the WT with the proposed controller are 18.9 rpm and 18.6 rpm when wind velocity changes from 13 m/s to 21 m/s and from 25 m/s to 32 m/s, respectively. In the same cases, the peak values with the raw controller are 19.7 rpm and 19.3 rpm; in that case, a fast shutdown would happen to the WT as a result of over-speed protection, which means that the WT would stop producing power and, even worse, the WT might be damaged from extreme loads. In this study, all supervisory controls for the WT are disabled for the sake of results comparison.

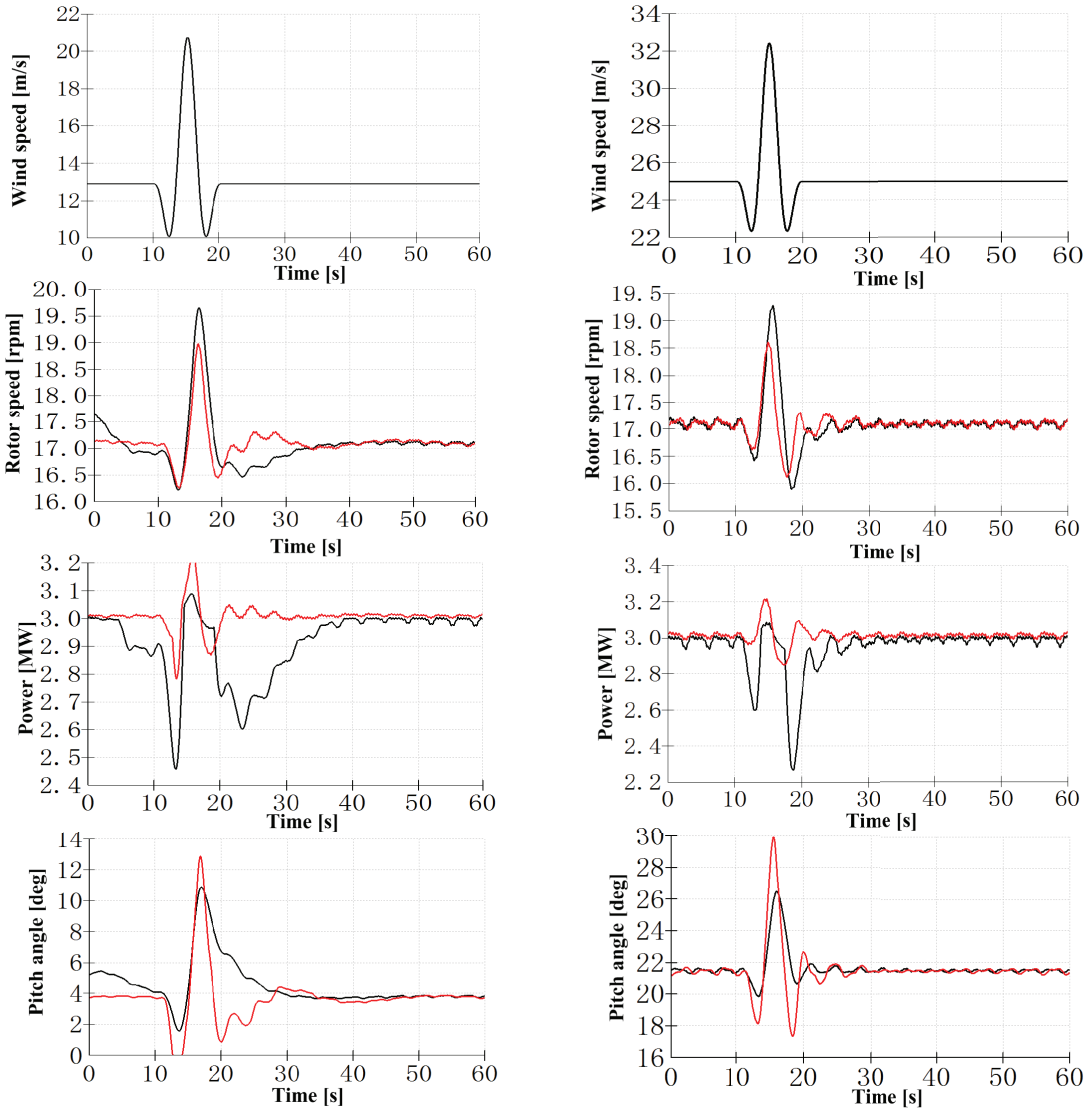

Figure 15. Simulation results under DLC 1.6 between raw controller and proposed controller (a) at wind speed of 13 m/s and (b) at wind speed of 25 m/s.

5.3.2. Results comparison between proposed controller and conventional strategy

Among simulation results, red curves and black ones are from the proposed controller and the controller improved by conventional strategy, respectively.

The simulation results at 12 m/s and 20 m/s mean wind speed are shown in Figures 16a and 16b, respectively. It can be seen that both updated controllers are responsible for transition and over-speed issues. The curves of blade 1 pitch angle and rotor speed are similar. This means that the rotor speed has been well regulated under turbulent winds by both controllers. However, the controller adopting the conventional strategy needs to be further improved in the aspect of producing maximum electrical power: at 20 m/s wind speed, there are still some points where electrical power deviates from full power.

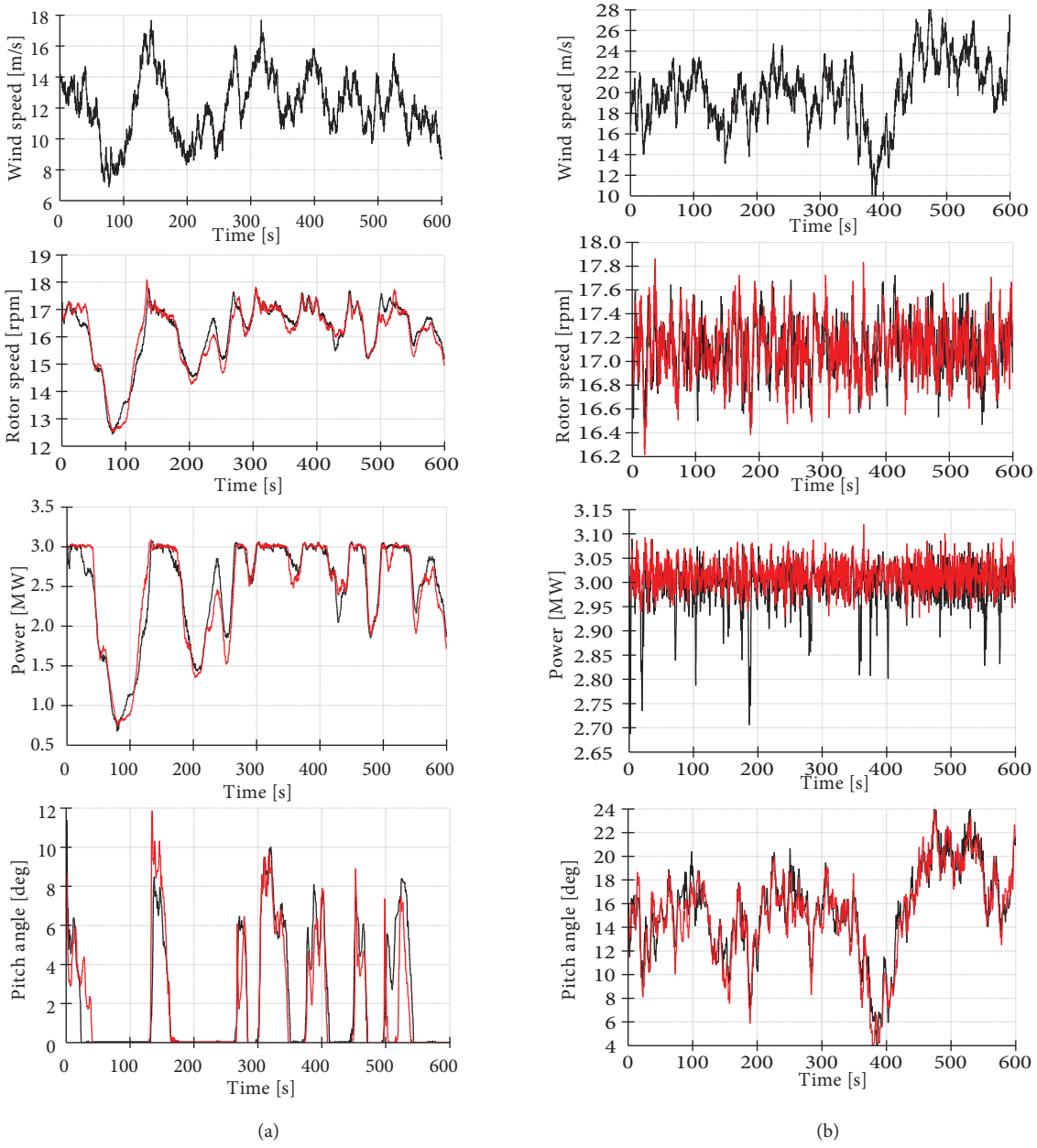

Figure 16. Simulation results under DLC 1.2 between conventional strategy and proposed controller (a) at wind speed of 12 m/s and (b) at wind speed of 20 m/s.

Figures 17a and 17b show simulation results under extreme operational gusts at 13 m/s and 25 m/s, respectively. When wind velocity changes from 13 m/s to 21 m/s and from 25 m/s to 32 m/s, the greatest values of rotor speed with the proposed controller are 18.9 rpm and 18.6 rpm, respectively. By comparison, the peak values of rotor speed under the controller updated by conventional strategy are slightly higherat 19.1 rpm and 18.8 rpm, respectively.

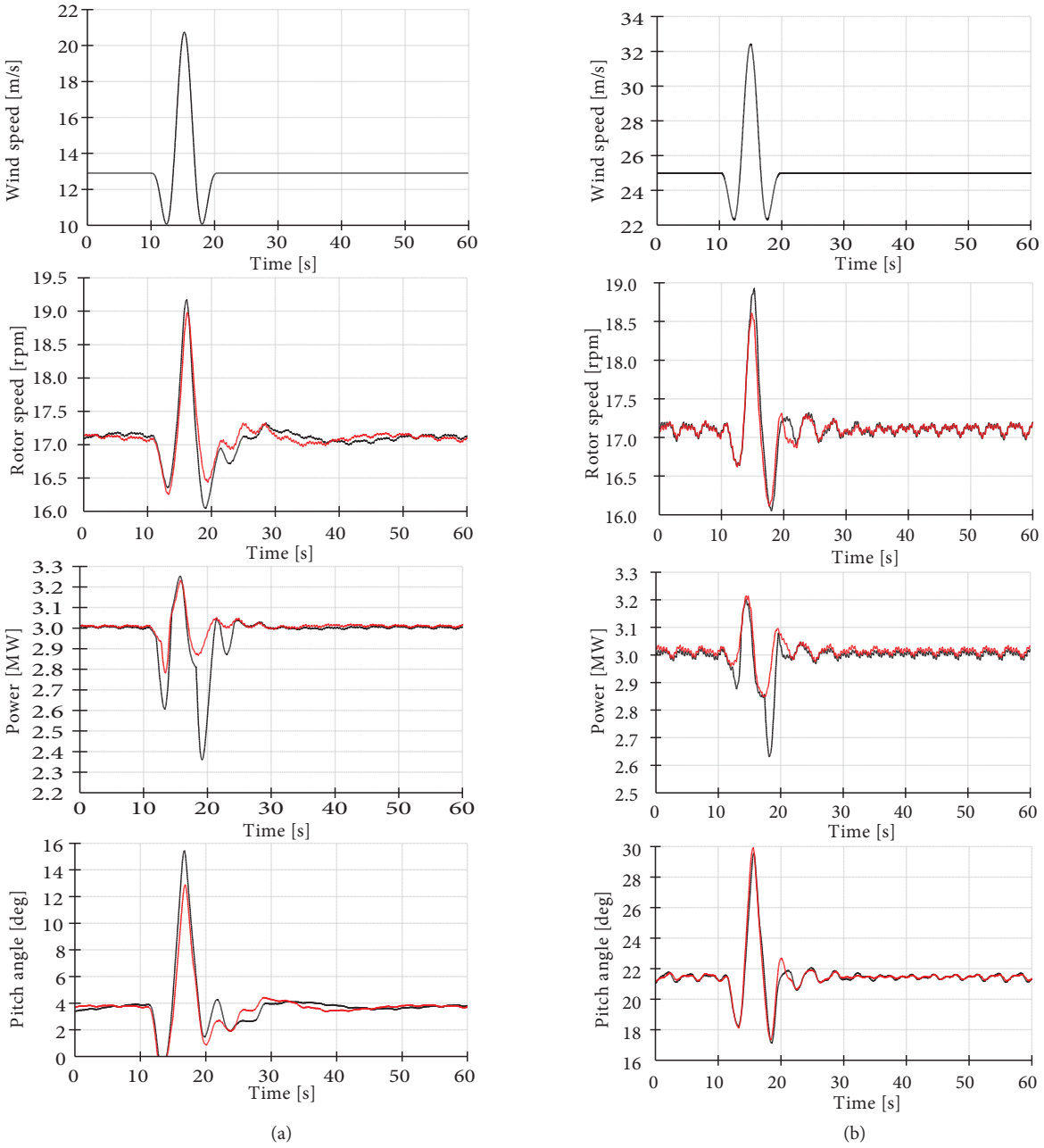

Figure 17. Simulation results under DLC 1.6 between conventional strategy and proposed controller (a) at wind speed of 13 m/s and (b) at wind speed of 25 m/s.

6. Conclusions

As an energy conversion system, a WT's primary objectives are to produce maximum electrical power and avoid equipment overloads. The conventional MBC is capable of satisfying general performance requirements. However, the transition issue between the TC and PC and the over-speed problem are not handled by MBC. Considering the electrical power output and rotor speed stability performance, the original controller is inferior to the two updated controllers and the proposed FLC solution outweighs the conventional strategy.

Under 20 m/s normal turbulent wind, the output electrical power under the original controller is loose and ranges from 2.2 MW to 3.1 MW, and the values of rotor speed are scattered between 15.7 rpm and 18.5 rpm. By comparison, after improvement by the conventional strategy, the produced power becomes denser and ranges between 2.7 MW and 3.1 MW, and the values of rotor speed converge in the region of 16.5–17.7 rpm. With the proposed solution, the output power further concentrates between 2.95 MW and 3.1 MW, and the values of rotor speed are in a range of 16.4–17.7 rpm. As expected, maximum electrical power is obtained by the proposed solution: the average power calculated from simulation results for the original controller, conventional strategy, and proposed solution are 2.88 MW, 2.98 MW, and 3.01 MW, respectively.

Under extreme operational gusts, the maximum rotor speed under the raw controller is highest up to 19.7 rpm, which undoubtedly causes the machine to shut down. In contrast, both updated controllers result in safe rotor speed, which is lower than the cut-out rotor speed of 19.15 rpm. Moreover, it can be seen that the greatest value of rotor speed under FLC modules is slightly smaller than that with the conventional strategy.

Although better performance was observed, the proposed solution could be optimized by introducing type-2 FLC and could be auto-tuned by adaptive FLC, for which further studies have to be carried out. However, the proposed solution in this study has successfully classified the expert knowledge into a systematic FLC structure and is more convenient to apply to industry compared to other advanced FLC solutions.

Acknowledgments

The authors thank the CMYWP company for providing the application case of the work and colleagues in the control system department of CMYWP for their valuable suggestions.

References

[1] World Wind Energy Association. The World Wind Energy Association 2014 Half-Year Report. Bonn, Germany: WWEA, 2014.

[2] Shiyong L. Fuzzy Control, Neurocontrol and Intelligent Cybernetics. Harbin, China: Harbin Institute of Technology Press, 1998.

[3] Laks JH, Pao LY, Wright AD. Control of wind turbines: past, present, and future. In: 2009 American Control Conference; 10–12 June 2009; St. Louis, Missouri, USA. New York, NY, USA: IEEE. pp. 2096–2103.

[4] Pao LY, Johnson KE. Control of wind turbines approaches, challenges, and recent developments. IEEE Contr Syst Mag 2011; 31: 44–62.

[5] Hand MM, Balas MJ. Systematic Controller Design Methodology for Variable-Speed Wind Turbines. Technical Report. Golden, CO, USA: National Renewable Energy Laboratory, 2002.

[6] Hansen MH, Hansen A, Larsen TJ. Control Design for a Pitch-Regulated Variable-Speed Wind Turbine. Report Riso-R-1500(EN). Roskilde, Denmark: Riso National Laboratory, 2005.

[7] Wright AD. Modern Control Design for Flexible Wind Turbines. Technical Report. Golden, CO, USA: National Renewable Energy Laboratory, 2004.

[8] Wright AD, Fingersh LJ. Advanced Control Design for Wind Turbines. Technical Report. Golden, CO, USA: National Renewable Energy Laboratory, 2008.

[9] Miller NW, Sanchez-Gasca JJ, Price WW, Delmerico RW. Dynamic modeling of GE 1.5 and 3.6 MW wind turbine-generators for stability simulations. In: IEEE 2003 Power Engineering Society General Meeting; 13–17 July 2003; Toronto, Canada. New York, NY, USA: IEEE. pp. 1977–1983.

[10] Bossanyi EA. The design of closed loop controllers for wind turbines. Wind Energy 2000; 3: 149–163.

[11] Bossanyi EA. Individual blade pitch control for load reduction. Wind Energy 2003; 6: 119–128.

[12] Bossanyi EA. Wind turbine control for load reduction. Wind Energy 2003; 6: 229–244.

[13] Bossanyi EA, Witcher D. Controller for 5MW reference turbine. Technical Report. Project UpWind. Bristol, UK: UpWind, 2009.

[14] Butterfield S, Musial W, Scott G. Definition of a 5-MW Reference Wind Turbine for Offshore System Development. Technical Report. Golden, CO, USA: National Renewable Energy Laboratory, 2009.

[15] Bossanyi EA, Ramtharan G, Savini B. The importance of control in wind turbine design and loading. In: 2009 17th Mediterranean Conference on Control and Automation; 24–26 June 2009; Thessaloniki, Greece. New York, NY, USA: IEEE. pp. 1269–1274.

[16] Altaş İH. Fuzzy logic control for a wind/battery renewable energy production system. Turk J Electr Eng Co 2012; 20: 187–206.

[17] Jabr HM, Lu D, Kar NC. Design and implementation of neuro-fuzzy vector control for wind-driven doubly-fed induction generator. IEEE T Sustain Energ 2011; 2: 404–413.

[18] Salim OM, Zohdy MA, Abdel-Aty-Zohdy H, Dorrah HT, Kamel AM. Type-2 fuzzy logic pitch controller for wind turbine rotor blades. In: Proceedings of the 2011 IEEE National Aerospace and Electronics Conference; 20–22 July 2011; Dayton, OH, USA. New York, NY, USA: IEEE. pp. 32–38.

[19] Chiang MH. A novel pitch control system for a wind turbine driven by a variable-speed pump-controlled hydraulic servo system. Mechatronics 2011; 21: 753–761.

[20] Sheikhan M, Shahnazi R, Yousefi AN. An optimal fuzzy PI controller to capture the maximum power for variable-speed wind turbines. Neural Comput Appl 2013; 23: 1359–1368.

[21] Bououden S, Chadli M, Filali S, El Hajjaji A. Fuzzy model based multivariable predictive control of a variable speed wind turbine: LMI approach. Renew Energ 2012; 37: 434–439.

[22] Calderaro V, Galdi V, Piccolo A, Siano P. A fuzzy controller for maximum energy extraction from variable speed wind power generation systems. Electr Pow Syst Res 2008; 78: 1109–1118.

[23] Oguz Y, Guney I. Adaptive neuro-fuzzy inference system to improve the power quality of variable-speed wind power generation system. Turk J Electr Eng Co 2010; 18: 625–646.

[24] Johnson KE. Adaptive Torque Control of Variable Speed Wind Turbines. Technical Report. Golden, CO, USA: National Renewable Energy Laboratory, 2004.

[25] Bongers PM. Modeling and identification of flexible wind turbines and a factorizational approach to robust control. PhD, Delft University of Technology, Delft, the Netherlands, 1994.

[26] Wang N, Johnson KE, Wright AD. Comparison of strategies for enhancing energy capture and reducing loads using LIDAR and feedforward control. IEEE T Contr Syst T 2013; 21: 1129–1142.

[27] Schlipf D, Cheng PW. Flatness-based feedforward control of wind turbines using Lidar. In: 19th World Congress of the International Federation of Automatic Control; 24–29 August 2014; Cape Town, South Africa. New York, NY, USA: IEEE. pp. 5820–5825.

[28] Abdullah MA, Yatim AHM, Tan CW, Saidur R. A review of maximum power point tracking algorithms for wind energy systems. Renew Sust Energ Rev 2012; 16: 3220–3227.

[29] Hu S. The Automatic Control Principle (Revised Version). Beijing, China: Science Press, 2008.

[30] Bianchi F, De Battista H, Mantz R. Wind Turbine Control Systems: Principles, Modelling and Gain-Scheduling Design. Berlin, Germany: Springer, 2006.

[31] Precup RE, Hellendoorn H. A survey on industrial applications of fuzzy control. Comput Ind 2011; 62: 213–226.

[32] Bossanyi EA. GH bladed version 4.3 user manual. Bristol, UK: Garrad Hassan and Partners Ltd., 2012.

[33] International Electrotechnical Commission. IEC 61400-1 International Standard (Third Edition), Wind Turbines – Part 1: Design Requirements. Geneva, Switzerland: IEC, 2005.